



Selective metal leaching from technosols based on synthetic root exudate composition

Hussein Kanbar, Zeinab Matar, Ghina Abed-Alhadi Safa, Veronique Kazpard

► To cite this version:

Hussein Kanbar, Zeinab Matar, Ghina Abed-Alhadi Safa, Veronique Kazpard. Selective metal leaching from technosols based on synthetic root exudate composition. *Journal of Environmental Sciences*, 2020, 96, pp.85-92. 10.1016/j.jes.2020.04.040 . hal-03317781

HAL Id: hal-03317781

<https://hal.science/hal-03317781>

Submitted on 28 Dec 2022

HAL is a multi-disciplinary open access archive for the deposit and dissemination of scientific research documents, whether they are published or not. The documents may come from teaching and research institutions in France or abroad, or from public or private research centers.

L'archive ouverte pluridisciplinaire **HAL**, est destinée au dépôt et à la diffusion de documents scientifiques de niveau recherche, publiés ou non, émanant des établissements d'enseignement et de recherche français ou étrangers, des laboratoires publics ou privés.

Selective metal leaching from technosols based on synthetic root exudate composition

Hussein Jaafar Kanbar^{1,2,**}, Zeinab Matar^{1,3,4,**}, Ghina Safa^{1,3}, Veronique Kazpard^{1,3,4}

1. Research and Analysis Platform for Environmental Sciences (PRASE), Doctoral School of Sciences and Technology (EDST), the Lebanese University, P.O. 5, Rafic Hariri Campus, Hadat, Lebanon.
2. Department of Chemistry, Umeå University, SE-901 87, Umeå, Sweden.
3. Department of Earth and Life Sciences, Faculty of Sciences, the Lebanese University, Rafic Hariri Campus, Hadat, Lebanon.
4. Laboratory of Georessources, Geosciences and Environment (L2GE), Faculty of Sciences, the Lebanese University, Fanar, Lebanon.

Received 16 February 2020

Revised 13 April 2020

Accepted 24 April 2020

Abstract: This study focused on metal release from technosols induced by synthetic root exudate (SRE). The effect of SRE composition on metal release was studied using six technosols. This was done by treating the technosols with SRE solutions having varying concentrations of low molecular weight organic acids (LMWOAs), namely oxalic, citric, and malic acids. Consequently, the physico-chemical parameters (pH and electric conductivity), Ca, Mg, Fe, Zn, and Cu release (by atomic absorption spectroscopy, AAS), chemical changes (by Fourier transform infrared, FTIR), and organic parameters (by fluorescence) were investigated. Metal release showed to be dependent on the SRE composition and technosol characteristics. Citric acid selectively released Ca, Mg, Zn, and Cu from technosols in a concentration-dependent manner; oxalic acid showed a significant role in the release of Mg and Fe. Under relatively high LMWOA concentrations, particulate organo-mineral complexes precipitated. Additionally, technosol weathering was seen by the dissolution of humic substances and ferriallophanes, which in turn caused metal release. However, re-precipitation of these phases showed to re-sorb metals, thus underestimating the role of LMWOAs in metal release. Therefore, the selective metal leaching was highly dependent on the SRE composition and LMWOA concentrations on one hand, and on the mineral, organic, and organo-mineral components of the technosols on the other. The understanding of such processes is crucial for

proposing and implementing environmental management strategies to reduce metal leaching or for the beneficial re-usage of metals (e.g., for agromining) from technosols.

Keywords:

Technosols

Oxalic acid

Citric acid

Metals

Desorption

Organo-mineral complexes

** These authors contributed equally to this work. Corresponding authors. E-mail: Hussein.kanbar@umu.se (H.J. Kanbar), z.matar@ul.edu.lb (Z. Matar).

Introduction

The production of anthropogenic materials is increasing worldwide due to urbanization and consequent development of industrial activities. This results in the formation of soils rich in organic and inorganic technogenic materials, i.e., technosols (e.g., De Kimpe and Morel, 2000). Studies focusing on the processes that occur in technosols, such as aging (Huot et al., 2013), formation of new minerals or organo-mineral complexes (Huot et al., 2014), and leaching of metals (Kanbar et al., 2018), have been reported in the literature. Moreover, technosol rehabilitation is a beneficial way of dealing with such materials. Indeed, technosols can be used as agricultural amendments (Paz-Ferreiro et al., 2014) or for metal mining via phytomining/agromining (Van der Ent et al., 2018), both resulting in profitable and environmentally safe results. These proposed solutions are based on selective metal extraction, leaching, or uptake (Do Nascimento and Xing, 2006), which in turn depend on complex interactions occurring between technosols and plant exudates (e.g., Badri and Vivanco, 2009). Plants release root exudates to cope in toxic environments by leaching undesirable or potentially harmful metals. Nonetheless, under nutrient-deficiency conditions, root exudates help in nutrient uptake (Chen et al., 2017). Accordingly, either bio-available or non-available metal complexes are formed. The composition and concentration of root exudates depend on the state of the plant, such as age, species, and draught level (Do Nascimento and Xing, 2006). However, root exudates generally contain sugars, amino acids, phenolic acids, and low molecular weight

organic acids (LMWOAs). The LMWOAs are the main components involved in metal behavior, mainly citric, succinic, malic, and oxalic acids (Agnello et al., 2014). The behavior of metals or nutrients depends on the physico-chemical, organic, metal, and mineral characteristics of technosols (Kanbar et al., 2018). Weathering of mineral surfaces (Kanbar and Kaouk, 2019) and forming dissolved or particulate organo-mineral complexes (Violante and Caporale, 2015) are some of the processes that depict metal behavior. Therefore, metal behavior in matrices, including technosols, can only be understood by taking into consideration these changes in addition to the SRE characteristics (composition and concentration). Studies that focus on the effect of synthetic root exudate (Huang et al., 2017) and individual LMWOAs, such as oxalic acid and citric acid (Chen et al., 2017; Song et al., 2016), on metal release have been reported in the literature. Nonetheless, rarely are the physico-chemical, mineral, chemical, and organic changes of the matrix linked to SRE composition and concentrations, especially in technosols. Therefore, this study aims to highlight the effects of individual LMWOAs, as part of a complex SRE, on metal behavior in technosols. Additionally, the processes undergoing in the liquid (SRE) and solid phases (technosols) were followed by the physico-chemical, mineral, and organic changes caused by SREs having different LMWOA composition and concentrations. Combining the results of the dissolved and particulate phases will help in understanding the behavior of metals in technosols. Consequently, treatment or the beneficial utilization of technosols, such as mining for precious metals (agromining), will be feasible.

1 Materials and methods

Metal desorption experiments were conducted on six technosols collected from the Lebanese seashore. The technosols were named NS1, NS4, NS9, FS11, FS14, and FS17. Information about sampling location and treatment, technosol characteristics (physico-chemical, mineral, chemical, and organic), total and oxalate extractable metals, and the role of organic matter on metal behavior are found elsewhere (Kanbar et al., 2018).

1.1 Synthetic root exudate composition

Seven synthetic root exudate solutions of various LMWOA concentrations were used to study metal behavior in the technosols. It should be noted that the composition of root exudates and their concentrations largely depend on soil type, nutrient availability, metal toxicity, drought condition, microbiome, plant species, and others (Bowsher et al., 2016). The normal SRE

composition used in this study, named “S”, was based on Huang et al. (2017). This SRE was proven to selectively desorb metals (Kanbar and Kaouk, 2019). The other 6 SRE solutions had different concentrations of oxalic acid (OA), citric acid (CA), and malic acid (MA) since these LMWOAs are the main components depicting metal behavior. S_{-OA} and S_{-CA} are similar to S except for the absence of OA and CA, respectively; S_{+OA}, S_{+CA}, and S_{+MA} are similar to S except for 5-fold concentrations of OA, CA, and MA, respectively; S_{5X} is 5 times more concentrated than S. The exact concentrations are included in **Appendix A (Table S1)**.

1.2 Metal desorption experiment

Each of the six technosols was treated with seven SRE solutions. A control sample (named Ctr) was run for each technosol using ultrapure water instead of SRE. 50 mL of each SRE solution was added to 200 mg of each technosol. The samples, run as triplicates, were shaken in an end-over-end shaker for 24 hr under ambient room temperature; negative controls were also run (i.e., just SRE solutions). The samples were then filtered using 0.45 µm filters and the pH and EC values were recorded (pH_f and EC_f); the pH and EC of the initial SRE solutions were also recorded (pH_i and EC_i). The pH values are reported as ΔpH (ΔpH= pH_f - pH_i). After the experiment, the technosols were freeze-dried before FTIR analysis (Fourier transform infrared). Furthermore, the filtered solutions were used for fluorescence spectrophotometry, FTIR, and atomic absorbance spectroscopy (AAS). The samples were acidified (by 1% HNO₃) before metal quantification (Ca, Mg, Fe, Zn, and Cu) by AAS (Rayleigh WFX-210; Shimadzu, China). Quality assurance and quality control (QA/QC) procedures are included in **Appendix A (S1)**.

1.3 Fourier transform infrared

The chemical changes of the solid (technosols) and liquid (SRE solutions) samples after the metal desorption experiment were determined by FTIR (FTIR-6300, JASCO, USA). The samples were prepared in KBr and the spectra were collected between 4000 and 400 cm⁻¹. The raw FTIR spectra were treated and normalized using the open-source MCR-ALS GUI provided by the Vibration Spectroscopy Core Facility at Umeå University (www.umu.se/en/research/infrastructure/visp/downloads/).

1.4 Fluorescence spectroscopy

The organic characteristics of the initial and final SRE solutions were detected by fluorescence spectroscopy (Fluorescence spectrophotometer F-7000, Hitachi, Japan). The spectra were recorded by a Fluorolog fluorescence spectrophotometer equipped with both excitation and

emission monochromators. A 150-W Xenon arc lamp was used as the excitation source. A complete representation of the fluorescence spectra was presented in the form of an excitation-emission matrix (EEM). The samples were placed in 1 cm optical path quartz cells and thermostated at 20°C. The 3D fluorescence spectra were obtained by increasing the excitation wavelengths from 240 to 600 nm (5 nm intervals) and emission wavelengths from 320 to 550 nm (2 nm intervals). The scan speed was set to 240 nm/min. The parameters were based on Lefevre et al. (2013). The final spectra were produced after subtraction from ultrapure water spectra (blank). The fluorescence intensities are given in arbitrary units.

2 Results and discussion

2.1 Physico-chemical changes induced by SREs

The pH values of the initial SRE solutions depended on the composition and concentrations of the organic acids (based on the pKa values of the carboxyl groups). The pH_f values changed due to the chemical, mineral, and organic composition of the technosols. For example, the pH_f of S_{+OA} treated samples did not show the lowest pH (or ΔpH, **Fig. 1a**) even though OA was the strongest acid among the other LMWOAs (based on pKa, **Table S1**). However, the carboxyl groups of OA deprotonated first. The influence of amino acids and phenolic acids on pH variation was not discussed since their concentrations were similar in all the SRE solutions. The pH_i and pH_f values ranged between 2.7-3.6 and 6-8, respectively (**Table S2**). The pH_f values (or ΔpH) of the technosols treated with relatively high LMWOA concentrations (i.e., S_{+OA}, S_{+CA}, S_{+MA}, and S_{5X}) were lower than samples treated with S (**Fig. 1a**). Moreover, there was no direct correlation between pH and LMWOA concentrations. S_{-OA} showed lower ΔpH values in comparison to S_{+OA}, indicating higher acidity for the treatments with lower OA concentrations; the same applied to CA treated samples (i.e., S_{-CA} and S_{+CA}). This unexpected variation might be explained by the formation of organo-mineral complexes, incomplete dissolution or dissociation of the added organic components, or the dissolution of humic substances from the technosols (Agnello et al., 2014; Drever and Vance, 1994) when LMWOA concentrations exceeded a certain limit (2 mmol/L for S_{+OA} and S_{+CA} in this case, **Table S1**). This was further supported by the fact that S_{5X} treated samples did not show the lowest ΔpH values. In general, the different SRE solutions, and not the technosols, explained the variation in pH as well as EC. Unlike pH, EC was linked to the LMWOA concentrations in the SRE solutions (**Fig. S1**). Indeed, the EC_f values increased in the following order: S_{-OA} and S_{-CA} (294-370 μS/cm), S (353-429 μS/cm), S_{+OA}, S_{+MA}, S_{+CA} (368-580 μS/cm), and S_{5X} (715-880 μS/cm) (**Fig. 1b**); the concentrations of the LMWOAs were 0.75, 1, 2, and 5 mmol/L, respectively (**Table S1**). Due

to the different processes occurring in the mixture, such as sorption/desorption of metals and or dissolution/precipitation of phases, there was no linear correlation between the LMWOA concentrations and EC. Even though the initial NS technosols had higher electric conductivity than the FS technosols (Kanbar et al., 2018), this was not the case after mixing with the SRE solutions. The initial EC values are included in **Table S2**.

2.2 Release of major cations by LMWOAs in a concentration-dependent manner

The release of the major cations, Ca and Mg, varied between the different treatments but not among technosols (**Fig. 2a and b**). The technosols treated with S_{+CA}, S_{+MA}, and S_{5X} had the highest Ca release, partially due to the dissolution of Ca-containing carbonates; the presence of carbonates was proven by X-ray diffraction (Kanbar et al., 2018). Indeed, Oelkers et al. (2011) evidenced that citrate (>0.1 mmol of citrate per kg of carbonate) significantly increased carbonate dissolution. In our case, 0.25 and 1.25 mmol/L of citric acid (S and S_{+CA}, respectively) showed a significant role in Ca release; this was not seen when CA concentrations were below 0.25 mmol/L (i.e., between S_{-CA} and S). Even though FS17 had the lowest initial Ca content among the other technosols (**Table S3**), it did not show the lowest Ca release, indicating that the initial Ca content is not linked to Ca release in this case. Therefore, and in addition to Ca-carbonate dissolution and incorporated Ca release (e.g., inner-sphere complexes), weakly bound Ca onto mineral and organic/humic surfaces and hydrated Ca was also released by SRE (e.g., Kanbar and Kaouk, 2019). On that note, ultrapure water treated technosols (Ctr) also showed Ca release (~0.1-0.6%). It is worth noting that Ca release was similar regardless of OA concentration (Ca release for S_{-OA}~S~S_{+OA}). The processes explaining Ca release also applied to Mg. Moreover, S_{+MA} and S_{+CA} treated technosols showed similar contents of Ca and Mg release, possibly due to similar pK_a values (**Table S1**), assuming similar dissociation, carboxyl group deprotonation, and major cation binding. Furthermore, the Mg released contents increased in the following order: S_{-OA} and S_{-CA}, S, S_{+OA}, S_{+CA}, and S_{+MA}, and finally S_{5X}. The metal release was linked to higher conductivity, salinity, and ionic strength (e.g., Du Laing et al., 2009); this was seen in the case of Mg and Ca (**Fig. S1**), but not for the other metals. Finally, Ca release from the technosols was CA and MA-concentration dependent when the LMWOA concentrations were relatively high (1-2 mmol/L), while Mg release was CA and OA-concentration dependent when the LMWOA concentrations ranged between 0.75 and 1 mmol/L. The magnitudes of metal release based on the SRE solutions are shown in **Fig. S2**.

2.3 Selective metal leaching from technosols

In contrast to the major cations (Mg and Ca), the release of Fe, Zn, and Cu was selective based on the composition of the technosols, SRE solutions, and the metals themselves (**Fig. 2c-e**). On the selectivity of the technosols, the NS samples showed the highest Fe release, the NS samples and FS11 showed the highest Zn release, and NS4 and NS9 showed the highest Cu release. The correlation between the released metals (Fe, Zn, and Cu) are included in **Fig. S1**. In all cases, S_{5X} showed the highest metal release; so, S_{5X} is not concerned in the discussion below. Iron was mainly released by S_{+OA} treatment, while Zn and Cu were mainly released by S_{+CA} treatment. Nonetheless, the other LMWOAs were also involved in the release of Fe, Zn, and Cu. The highest metal release was recorded for samples having the highest total metal and oxalate extractable metal contents. The percentages of the oxalate extractable metals for those samples (marked as bold in **Table S3**) averaged 65%, 66%, and 33%, for Fe, Zn, and Cu, respectively. Ferriallophanes or Fe-oxyhydroxides and oxalate extractable metals were the main causes of high metal release. Indeed, the dissolution of Fe-oxyhydroxides from the Fe-rich technosols was expected after mixing with SREs, even at neutral to alkaline pH (e.g., Chen et al., 2017); additionally, OA was proven to release Fe from Fe-bearing minerals (Pariyan et al., 2019). The effect of OA concentration on Fe release was seen between S_{-OA} and S_{+OA} treatments (i.e., between 0 and 1.25 mmol/L of OA), however, the variation was more prominent in the 0-0.25 mmol/L range (S/S_{-OA} > S_{+OA}/S, **Fig. S2**); the same applied to CA. The S and S_{+MA} treated technosols showed similar Fe content release. Interestingly, the absence of either OA or CA showed negligible Fe release in all the technosols (inset of **Fig. 2c**). This raises the question of complementarity between the different LMWOAs in some processes, such as forming available binding sites, binding to mineral/humic surfaces, changing degradation rate, desorbing metals, influencing physico-chemical parameters, and dissolving minerals (e.g., (Ström et al., 2001)).

Zinc was highly released from the technosols after SRE treatments, even for samples with relatively low initial Zn contents, namely FS14 and FS17 (inset of **Fig. 2d** and **Table S3**). This was caused by the formation of soluble complexes with dissolved organic matter (DOM) (e.g., Chen et al., 2017). Zinc release from the Zn-rich technosols (all NS samples and FS11) was due to the predominance of oxalate extractable Zn species (Kanbar et al., 2018). Interestingly, Zn release was OA and CA concentration-dependent in those technosols when the LMWOA concentrations ranged between 0 and 1.25 mmol/L. However, Zn release was more affected by CA than by OA, especially when the LMWOA concentrations were relatively low (S/S_{-CA} > S_{+CA}/S; **Fig. S2**). It was proven that DOM of plant exudates, specifically CA, readily sorb Zn (e.g., Song et al., 2016). Zinc release was similar between S_{+MA} and S_{+OA} treated samples, which

was lower than S_{+CA} treated ones. Calcium release, on the other hand, was similar between S_{+MA} and S_{+CA} treated samples. Therefore, the dissociation constants of the LMWOA functional groups were not directly linked to metal leaching in the technosols. Other processes depict metal release, such as the formation of organo-mineral complexes (as mentioned in the previous section).

Copper release depended on the LMWOA concentrations and components (**Fig. 2e**). It was proven that Cu has a high affinity for binding to organic components, such as CA (Song et al., 2016). Furthermore, it was shown that an SRE solution, similar to S in this study, desorbed surface-bound copper and dissolved Cu-minerals (Kanbar and Kaouk, 2019). Although not as clear as Zn and Fe release, Cu release was dependent on CA and OA when the LMWOA concentrations ranged between 0 and 1.25 mmol/L; yet it was more prominent in the 0.25-1.25 mmol/L range (**Fig. S2**). Regarding Cu release, MA and OA showed similar effects. Interestingly, Cu release was not LMWOA concentration-dependent in the NS1 and FS technosols. This might be because Cu has a high affinity for binding to OM (Matar et al., 2015), and the relatively low LMWOA concentrations were sufficient to release all extractable Cu. Even though NS4 and NS9 had similar Cu contents (total and oxalate extractable, **Table S3**), the role of LMWOAs on Cu release was more prominent for the former; NS4 showed higher variation in Cu release between S_{-OA} and S_{-CA} on one hand, and S_{+OA} and S_{+CA} on the other. This was linked to higher Fe-oxyhydroxides/ferrihallophanes contents in NS4 (as indicated by high oxalate extractable Fe contents, **Table S3**). Indeed, these iron phases might re-sorb released metals (Grybos et al., 2007), thus underestimating the role of LMWOAs on metal release.

2.4 Chemical changes of the technosols after SRE treatment and precipitation of organo-mineral complexes

2.4.1 Technosol FTIR spectra

The SRE-induced chemical changes of the technosols are compared; the FTIR spectra of the initial technosols are found elsewhere (Kanbar et al., 2018). In comparison to the initial technosol, the bands in the 800-450 cm⁻¹ region changed after SRE treatment, as shown by the peaks at 790, 612, and 530 cm⁻¹ (**Fig. 3a**). The S and S_{+OA} treated samples showed significant changes in that region; OA readily sorbed onto soils in general (Jagadamma et al., 2012) and Fe-rich minerals in particular (Bhatti et al., 1998), such as the case of the ferrihallophane-rich technosols. This suggested that the peak deformation in that spectral region was partially caused by OA. Other LMWOAs, such as CA, MA, and succinic acid, have a fingerprint in that region

as well (e.g., Huang et al., 2017). Moreover, the bands at 650-450 cm^{-1} might be due to $-\text{CH}_2$ vibration, possibly formed by LMWOAs (Huang et al., 2017) or by chemical interactions between the Al-O groups of aluminosilicates in the technosols (e.g., clays or allophanes) with $-\text{CH}$ groups of sugars in the SRE solutions (Bishop et al., 2013). The bands in the 600-400 cm^{-1} region also indicated Si-O bending vibrations (of silicates, aluminosilicates, and allophanes); these bands strongly rely on the octahedral atom (Madejová et al., 2017). Therefore, changes in the IR spectra in that region suggested mineral weathering caused by LMWOAs (Drever and Vance, 1994). On a similar note, the bands in the 850-600 cm^{-1} region indicated OH bending vibration of minerals, such as clays. In the case of surface complexation (organo-mineral complex), LMWOAs, such as OA and CA (Hayakawa et al., 2018), can weather minerals, consequently leading to spectral modification in the 850-600 cm^{-1} region (Madejová et al., 2017 and references cited therein).

The LMWOAs might cause the release of interlayer or inner-sphere metals from clays or organo-mineral complexes present in the technosols. On the formation of organo-mineral complexes, an ester group (C-O) emerged at 1318 cm^{-1} in the $\text{S}_{+\text{OA}}$ and $\text{S}_{5\text{X}}$ treated samples that had a strong technogenic character (**Fig. 3b**), i.e., NS1, NS4, NS9, and FS11; the other samples had a lithogenic nature (Kanbar et al., 2018). The ester group might have formed in the technosols due to SRE-induced weathering. Since this peak was only detected in samples treated with elevated OA concentrations and in certain technosols, it is believed that alcohol groups in OA weathered the carboxyl groups of humic substances or allophanes. Furthermore, the intensity of the 1729 cm^{-1} peak increased in all the treatments in comparison to the initial spectrum. Therefore, this peak, indicating carbonyl (C=O) of humic substances or LMWOAs (Huang et al., 2017), might have formed by weathering of the allophane-rich NS technosols, binding of LMWOAs onto technosols, or precipitation of organo-mineral complexes (Markich and Brown, 1999). The change in that peak can also be due to the degradation of the ester band (Arocena et al., 1995). Therefore, the possibly formed ester, as discussed previously, might be directly, yet partially, weathered.

The OM peaks at 1400 cm^{-1} (carboxyl stretching and O-H bending of carboxyl group), 1470-1400 cm^{-1} (aliphatic C-H bending), 1614 cm^{-1} ($-\text{C}-\text{O}$ stretching and O-H bending of humic carboxyl groups), 1640 cm^{-1} (aromatic C=C stretching), and $\sim 3400 \text{ cm}^{-1}$ (amine (N-H) stretching and OH stretching of humic substances) did not show a trend among the treatments (**Fig. 3b and c**). These peaks changed according to humic substance weathering, water content fluctuation, and organic or organo-mineral complex precipitation (Matar et al., 2015). However, the aliphatic C-H stretching peaks (at 2922 and 2852 cm^{-1}) decreased after suspension with SRE

as well as ultrapure water (inset in **Fig. 3c**) suggesting the dissolution, degradation, or weathering of organic matter.

2.4.2 FTIR spectra of the SRE solutions after metal desorption

The change in the IR spectra of the liquid samples after the metal desorption experiment marked the chemical changes of the dissolved phases (**Fig. 4**). All the samples and treatments showed a peak at 410 cm^{-1} , except for the S_{-CA} and S_{-OA} treated technogenic samples (i.e., NS samples). Hence, the disappearance of that peak was linked to allophane weathering or degradation when the LMWOA concentrations were relatively low (**Fig. 4a**). The precipitation of organo-mineral complexes from the LMWOAs and technosols was possible when the LMWOA concentrations were above 1 mmol/L (i.e., S_{+OA} , S_{+CA} , and S_{+MA}), thus reducing technosol weathering. Indeed, that would be a reason for higher alkalinity for S_{+OA} , S_{+CA} , and S_{+MA} treated technosols in comparison to the S_{-OA} and S_{-CA} treated ones (**Fig. 1a**). Nonetheless, organo-mineral complexes formed due to LMWOA-induced weathering. The higher EC of the high LMWOA solutions promoted complex formation (Newcomb et al., 2017), while the organic acids remained dissolved in the low LMWOA concentrated solutions. Similar results were found in the $600\text{--}400\text{ cm}^{-1}$ region (i.e., modified IR spectra for S_{-OA} and S_{-CA} treated technosols). The change in the IR fingerprint might be due to the dissolution of carbonates or other phases that were involved in buffering the solution. Furthermore, the fate of LMWOAs (e.g., dissolution, precipitation, or complexation) was dependent on several parameters, such as pH, EC, and mineral composition (e.g., Newcomb et al., 2017). This further supported the variation in the FTIR fingerprint for the different SRE-treated technosols. Another peak that emerged in the samples was 1730 cm^{-1} (**Fig. 4b**), possibly belonging to the carboxyl group, and more precisely the carbonyl group of LMWOAs. Once deprotonated, that peak disappeared and was replaced by a 1626 cm^{-1} peak (Iwase et al., 1999). Due to peak overlapping, this could not be verified in our case. However, the 1730 cm^{-1} peak was more prominent in the S_{+OA} , S_{+MA} , and S_{+CA} treated samples, suggesting that a part of these LMWOAs did not deprotonate, possibly due to oversaturation and consequent precipitation or organo-mineral complex formation. It should be noted that the organo-mineral complexes could be of various sizes (i.e., particulate or dissolved). On the same note, the peaks at $1640\text{--}1600\text{ cm}^{-1}$ ($C=C$, $C=O$, or $C-O$ of humic substance) and 3400 cm^{-1} (NH or OH of humic substances, **Fig. 4c**) were the lowest for samples treated with high LMWOA concentrations, suggesting that SRE solutions with low LMWOA concentrations had a bigger role in humic acid weathering.

2.5 LMWOA-induced changes on DOM and indications of organo-mineral complex precipitations: fluorescence

The 3D fluorescence EEM showed changes in two regions after suspension with SRE (**Fig. 5**). The first region showed two peaks, which were roughly centered at the $\lambda_{\text{ex}}/\lambda_{\text{em}}$ of 245-250/338 nm and 290-295/338 nm. These peaks were attributed to microbial by-product like materials, such as proteins and tryptophan. The second region was located in the $\lambda_{\text{ex}}/\lambda_{\text{em}}$ of 260-420/380-500 nm range and was attributed to humic acid (HA)-like substances (Chen et al., 2003). The maximum fluorescence intensities of these peaks, F_{max} , were obtained at fixed excitation wavelengths and are presented in **Fig. 5e** and **Table S4**. Only the humic acid-like region is discussed hereafter due to the link with the processes undergoing in the technosols. The protrusion of the HA-like region differed between treatments but not between the technosols; therefore, the EEM of one technosol is given (**Fig. 5a-d**). There was an enhancement in the HA-like region for samples treated with relatively high LMWOA concentrations, as seen between $S_{\text{-OA}}$ and S (**Fig. 5b-c** and **e**). This supported the role of SRE in technosol weathering and HA release when the LMWOA concentrations were low. Therefore, and similar to LMWOAs, HA had a role in releasing metals from the technosols. The change in the HA-like peaks was less obvious for higher LMWOA concentrations, i.e., between S and $S_{\text{+OA}}$ (**Fig. 5c-d**). Under those conditions, and as suggested by FTIR, precipitation of SRE components and formation of particulate organic matter or organo-mineral complexes occurred.

2.6 Discussion: chemical and organic processes occurring in the SRE-technosol mixture

The carboxyl groups of the LMWOAs (in the SRE solutions) deprotonated due to the rise in pH caused by the addition of technosols (**Fig. 1a**). Consequently, the dissolved LMWOAs triggered metal release from the technosols (e.g., Perelomov et al., 2011) or formed particulate or dissolved complexes with minerals, organics, or organo-minerals (Pan et al., 2010). Humic acids were also dissolved from the technosols via SRE-induced weathering or degradation (**Fig. 5**). Therefore, metals might form dissolved or particulate complexes with LMWOAs and HAs. Having a low carboxyl pKa (**Table S1**), OA was expected to be the first LMWOA to sorb metals. Indeed, OA showed the highest influence on Fe, Zn, and Cu release (**Fig. 2c-e**). However, CA has three carboxyl groups, while each of OA and MA has only two (**Table S1**). This might explain higher Zn and Cu release in $S_{\text{+CA}}$ treated technosols in comparison to the other SRE solutions (**Fig. 2**). Interestingly, CA showed a more significant role in metal chelating when OA was absent. This was seen by lower metal release for $S_{\text{-CA}}$ treated samples

in comparison to S_{-OA} treated ones (e.g., Cu and Zn). Double deprotonation of the carboxyl groups of MA occurred after sorption (Karageorgaki and Ernst, 2014). This indicated that even if CA has more carboxyl groups, MA has the same effect on chelating metals or forming organo-mineral complexes. This applied to the release of Ca, Mg, and Cu. Furthermore, organo-mineral complexes formed when the LMWOA concentrations were high. In those treatments, surface mineral weathering was promoted, leading to prolonged periods of metal release (>24 hr). Therefore, more interactions and processes will change the physico-chemical, chemical, mineral, and organic characteristics of the technosols. Accordingly, metal release continuous as long as the organic components (LMWOAs) are in contact with the technosols.

3 Conclusion

The synthetic root exudate-induced changes were studied on technosol characteristics (physico-chemical, mineral, organic, and chemical). Metal release from the technosols depended on the SRE composition (i.e., oxalic, citric, and malic acids), LMWOA concentration, and technosol composition (i.e., metal contents, ferriallorphanes, and humic substances). Indeed, the metal release was highly selective. For example, CA and MA showed significant Ca release only when the LMWOA concentrations were relatively high (S_{+CA} and S_{+MA}), while OA did not have a role in Ca release regardless of concentration. However, Mg release was dependent on OA and CA, mainly when the LMWOA concentrations were relatively low. On the other hand, the release of Fe, Zn, and Cu was more selective, especially between the different technosols. The selectivity of metal leaching by LMWOAs largely depended on the solubility of the LMWOAs and technosol composition. Indeed, organo-mineral complexes formed between the LMWOAs and technosol organic matter (humic materials), minerals, and organo-minerals, especially under relatively high LMWOA concentrations. Furthermore, the released metals, e.g., due to humic acid or ferriallorphane dissolution, might be re-sorbed by the precipitating organo-mineral complexes, therefore underestimating the role of LMWOAs on metal release. These findings highlight the different processes that depict metal behavior in heterogeneous technosols. Only when these notions are understood will it be possible to beneficially re-use technosols in sustainable management plans (e.g., agromining).

Acknowledgment

This work was financed by the research grant programs of the Lebanese University (le projet est soutenu par le programme de subvention de la recherche scientifique à l'Université Libanaise). The funding source had no involvement in the study design, writing of the report,

and decision to submit the article for publication. We thank Dr. Elias Maatouk (Laboratory of Georessources, Geosciences and Environment, L2GE) for flame photometry and EC measurements and the research assistants of the Research and Analysis Platform for Environmental Sciences (PRASE), namely Ms. Sahar Rihane and Ms. Malak Tofeily (FTIR), Ms. Manal Houhou-Hadada and Mr. Ali Berro (AAS), Ms. Marwa Fouani (Fluorescence), and Ms. Layal Hajjar and Mr. Mohammad Siblani (assistance in laboratory work).

Appendix A. Supplementary data

Supplementary data associated with this article can be found in the online version at xxxxxx.

References

- Agnello, A.C., Huguenot, D., Van Hullebusch, E.D., Esposito, G., 2014. Enhanced phytoremediation: A review of low molecular weight organic acids and surfactants used as amendments. *Crit. Rev. Environ. Sci. Technol.* 44(22), 2531–2576. <https://doi.org/10.1080/10643389.2013.829764>.
- Arocena, J.M., Pawluk, S., Dudas, M.J., Gajdostik, A., 1995. In situ investigation of soil organic matter aggregates using infrared microscopy. *Can. J. Soil Sci.* 75(3), 327–332. <https://doi.org/10.4141/cjss95-047>.
- Badri, D. V., Vivanco, J.M., 2009. Regulation and function of root exudates. *Plant, Cell Environ.* 32(6), 666–681. <https://doi.org/10.1111/j.1365-3040.2009.01926.x>.
- Bhatti, J.S., Comerford, N.B., Johnston, C.T., 1998. Influence of soil organic matter removal and pH on oxalate sorption onto a spodic horizon. *Soil Sci. Soc. Am. J.* 62(1), 152–158. <https://doi.org/10.2136/sssaj1998.03615995006200010020x>.
- Bishop, J.L., Ethbrampe, E.B., Bish, D.L., Abidin, Z.L., Baker, L.L., Matsue, N., et al., 2013. Spectral and hydration properties of allophane and imogolite. *Clays Clay Miner.* 61(1), 57–74. <https://doi.org/10.1346/CCMN.2013.0610105>.
- Bowsher, A.W., Ali, R., Harding, S.A., Tsai, C.J., Donovan, L.A., 2016. Evolutionary divergences in root exudate composition among ecologically-contrasting helianthus species. *PLoS One.* 11(1), 1–16. <https://doi.org/10.1371/journal.pone.0148280>.
- Chen, W., Westerhoff, P., Leenheer, J.A., Booksh, K., 2003. Fluorescence excitation–emission matrix regional integration to quantify spectra for dissolved organic matter. *Environ. Sci. Technol.* 37(24), 5701–5710. <https://doi.org/10.1021/es034354c>.
- Chen, Y.T., Wang, Y., Yeh, K.C., 2017. Role of root exudates in metal acquisition and tolerance. *Curr. Opin. Plant Biol.* 39, 66–72. <https://doi.org/10.1016/j.pbi.2017.06.004>.
- De Kimpe, C.R., Morel, J.-L., 2000. Urban soil management: a growing concern. *Soil Sci.* 165(1), 31–40.
- Do Nascimento, C.W.A., Xing, B., 2006. Phytoextraction: A review on enhanced metal availability and plant accumulation. *Sci. Agric.* 63(3), 299–311, <https://doi.org/10.1590/S0103-90162006000300014>.
- Drever, J.I., Vance, G.F., 1994. Role of soil organic acids in mineral weathering processes. In: Pittman, E.D., Lewan, M.D. (Eds.). *Organic Acids in Geological Processes*. Springer Berlin Heidelberg, Berlin, Heidelberg, pp. 138–161. https://doi.org/10.1007/978-3-642-78356-2_6.
- Du Laing, G., Rinklebe, J., Vandecasteele, B., Meers, E., Tack, F.M.G., 2009. Trace metal

behaviour in estuarine and riverine floodplain soils and sediments: A review. *Sci. Total Environ.* 407(13), 3972–3985. <https://doi.org/10.1016/j.scitotenv.2008.07.025>.

Grybos, M., Davranche, M., Gruau, G., Petitjean, P., 2007. Is trace metal release in wetland soils controlled by organic matter mobility or Fe-oxyhydroxides reduction? *J. Colloid Interface Sci.* 314(2), 490–501. <https://doi.org/10.1016/j.jcis.2007.04.062>

Hayakawa, C., Fujii, K., Funakawa, S., Kosaki, T., 2018. Effects of sorption on biodegradation of low-molecular-weight organic acids in highly-weathered tropical soils. *Geoderma*. 324, 109–118. <https://doi.org/10.1016/j.geoderma.2018.03.014>.

Huang, Y., Zhao, L., Keller, A.A., 2017. Interactions, transformations, and bioavailability of nano-copper exposed to root exudates. *Environ. Sci. Technol.* 51(17), 9774–9783. <https://doi.org/10.1021/acs.est.7b02523>.

Huot, H., Simonnot, M.-O., Marion, P., Yvon, J., De Donato, P., Morel, J.-L., 2013. Characteristics and potential pedogenetic processes of a Technosol developing on iron industry deposits. *J. Soils Sediments*. 13(3), 555–568. <https://doi.org/10.1007/s11368-012-0513-1>.

Huot, H., Simonnot, M.-O., Watteau, F., Marion, P., Yvon, J., De Donato, P., et al., 2014. Early transformation and transfer processes in a Technosol developing on iron industry deposits. *Eur. J. Soil Sci.* 65(4), 470–484. <https://doi.org/10.1111/ejss.12106>.

Iwase, T., Varotsis, C., Shinzawa-Itoh, K., Yoshikawa, S., Kitagawa, T., 1999. Infrared evidence for Cu B ligation of photodissociated CO of cytochrome c oxidase at ambient temperatures and accompanied deprotonation of a carboxyl side chain of protein. *J. Am. Chem. Soc.* 121(6), 1415–1416. <https://doi.org/10.1021/ja983242w>.

Jagadamma, S., Mayes, M.A., Phillips, J.R., 2012. Selective sorption of dissolved organic carbon compounds by temperate soils. *PLoS One*. 7(11), e50434. <https://doi.org/10.1371/journal.pone.0050434>.

Kanbar, H.J., Kaouk, M., 2019. Mineral and chemical changes of sediments after Cu sorption and then desorption induced by synthetic root exudate. *Chemosphere*. 236, 124393. <https://doi.org/10.1016/j.chemosphere.2019.124393>.

Kanbar, H.J., Srouji, E.E., Zeidan, Z., Chokr, S., Matar, Z., 2018. Leaching of metals in coastal technosols triggered by saline solutions and labile organic matter removal. *Water, Air, Soil Pollut.* 229(5), 157. <https://doi.org/10.1007/s11270-018-3808-z>.

Karageorgaki, C., Ernst, K.-H., 2014. A metal surface with chiral memory. *Chem. Commun.* 50(15), 1814–1816. <https://doi.org/10.1039/C3CC48797K>.

Lefevre, G.H., Hozalski, R.M., Novak, P.J., 2013. Root exudate enhanced contaminant

desorption: An abiotic contribution to the rhizosphere effect. *Environ. Sci. Technol.* 47(20), 11545–11553. <https://doi.org/10.1021/es402446v>.

Madejová, J., Gates, W.P., Petit, S., 2017. IR spectra of clay minerals. In: Gates, W.P., Klopogge, J.T., Madejová, J., Bergaya, F. (Eds.). *Developments in Clay Science*. Eslevier, pp. 107–149. <https://doi.org/10.1016/B978-0-08-100355-8.00005-9>.

Markich, S.J., Brown, P.L., 1999. Thermochemical data for environmentally-relevant elements. Australian Nuclear Science and Technology Organisation, Australian Nuclear Science and Technology Organisation (ANSTO). E-report, Menai, Australia.

Matar, Z., Soares Pereira, C., Chebbo, G., Uher, E., Troupel, M., Boudahmane, L., et al., 2015. Influence of effluent organic matter on copper speciation and bioavailability in rivers under strong urban pressure. *Environ. Sci. Pollut. Res.* 22(24), 19461–19472. <https://doi.org/10.1007/s11356-015-5110-6>.

Newcomb, C.J., Qafoku, N.P., Grate, J.W., Bailey, V.L., De Yoreo, J.J., 2017. Developing a molecular picture of soil organic matter–mineral interactions by quantifying organo–mineral binding. *Nat. Commun.* 8(1), 396. <https://doi.org/10.1038/s41467-017-00407-9>.

Oelkers, E.H., Golubev, S. V., Pokrovsky, O.S., Bénézech, P., 2011. Do organic ligands affect calcite dissolution rates? *Geochim. Cosmochim. Acta.* 75(7), 1799–1813. <https://doi.org/10.1016/j.gca.2011.01.002>.

Pan, B., Tao, S., Dawson, R.W., Xing, B.S., 2010. Formation of organo-mineral complexes as affected by particle size, pH, and dry - wet cycles. *Soil Res.* 48(8), 713–719. <https://doi.org/10.1071/SR10029>.

Pariyan, K., Hosseini, M.R., Ahmadi, A., Zahiri, A., 2019. Optimization and kinetics of oxalic acid treatment of feldspar for removing the iron oxide impurities. *Sep. Sci. Technol.* 1–12. <https://doi.org/10.1080/01496395.2019.1612913>.

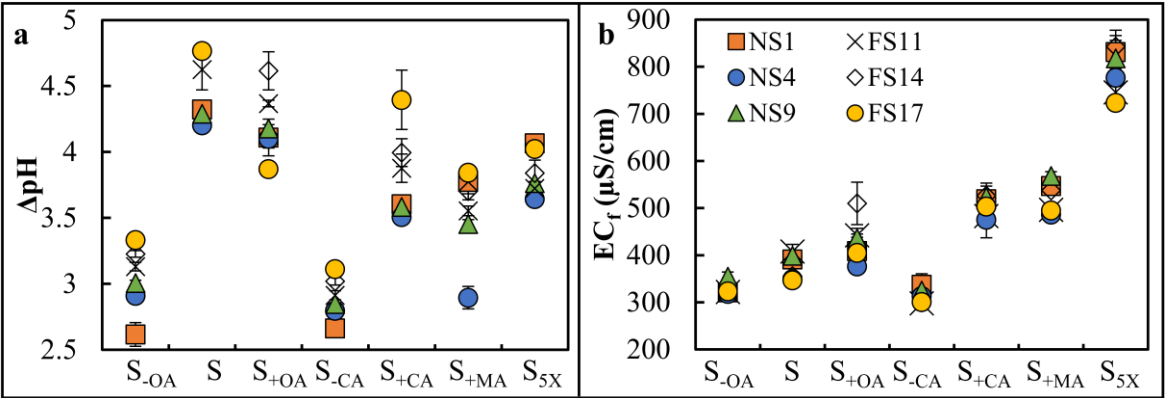
Paz-Ferreiro, J., Lu, H., Fu, S., Méndez, A., Gascó, G., 2014. Use of phytoremediation and biochar to remediate heavy metal polluted soils: A review. *Solid Earth.* 5(1), 65–75. <https://doi.org/10.5194/se-5-65-2014>.

Perelomov, L. V., Pinskiy, D.L., Violante, A., 2011. Effect of organic acids on the adsorption of copper, lead, and zinc by goethite. *Eurasian Soil Sci.* 44(1), 22–28. <https://doi.org/10.1134/S1064229311010091>.

Song, Y., Ammami, M., Benamar, A., Mezazigh, S., Wang, H., 2016. Effect of EDTA, EDDS, NTA and citric acid on electrokinetic remediation of As, Cd, Cr, Cu, Ni, Pb and Zn contaminated dredged marine sediment. *Environ. Sci. Pollut. Res.* 23(11), 10577–10586. <https://doi.org/10.1007/s11356-015-5966-5>.

520 Ström, L., Owen, A.G., Godbold, D.L., Jones, D.L., 2001. Organic acid behaviour in a
521 calcareous soil: Sorption reactions and biodegradation rates. *Soil Biol. Biochem.* 33(X),
522 2125–2133. [https://doi.org/10.1016/S0038-0717\(01\)00146-8](https://doi.org/10.1016/S0038-0717(01)00146-8).
523 Van der Ent, A., Echevarria, G., Baker, A.J.M., Morel, J.L., (Editors), 2018. *Agromining:
524 Farming for Metals*. Springer Book. <https://doi.org/10.1007/978-3-319-61899-9>.
525 Violante, A., Caporale, A.G., 2015. Biogeochemical processes at soil-root interface. *J. Soil Sci.
526 Plant Nutr.* 15(2), 422–448. <https://doi.org/10.4067/s0718-95162015005000038>.
527
528

529 **List of figures**



532 **Fig. 1** The variation of ΔpH (a) and EC_f (b) for the SRE solutions after mixing with the
533 technosols. For a clearer representation of the graphs, the initial values are not included here;
534 pH_i , pH_f , and EC_i are reported in **Table S2**.

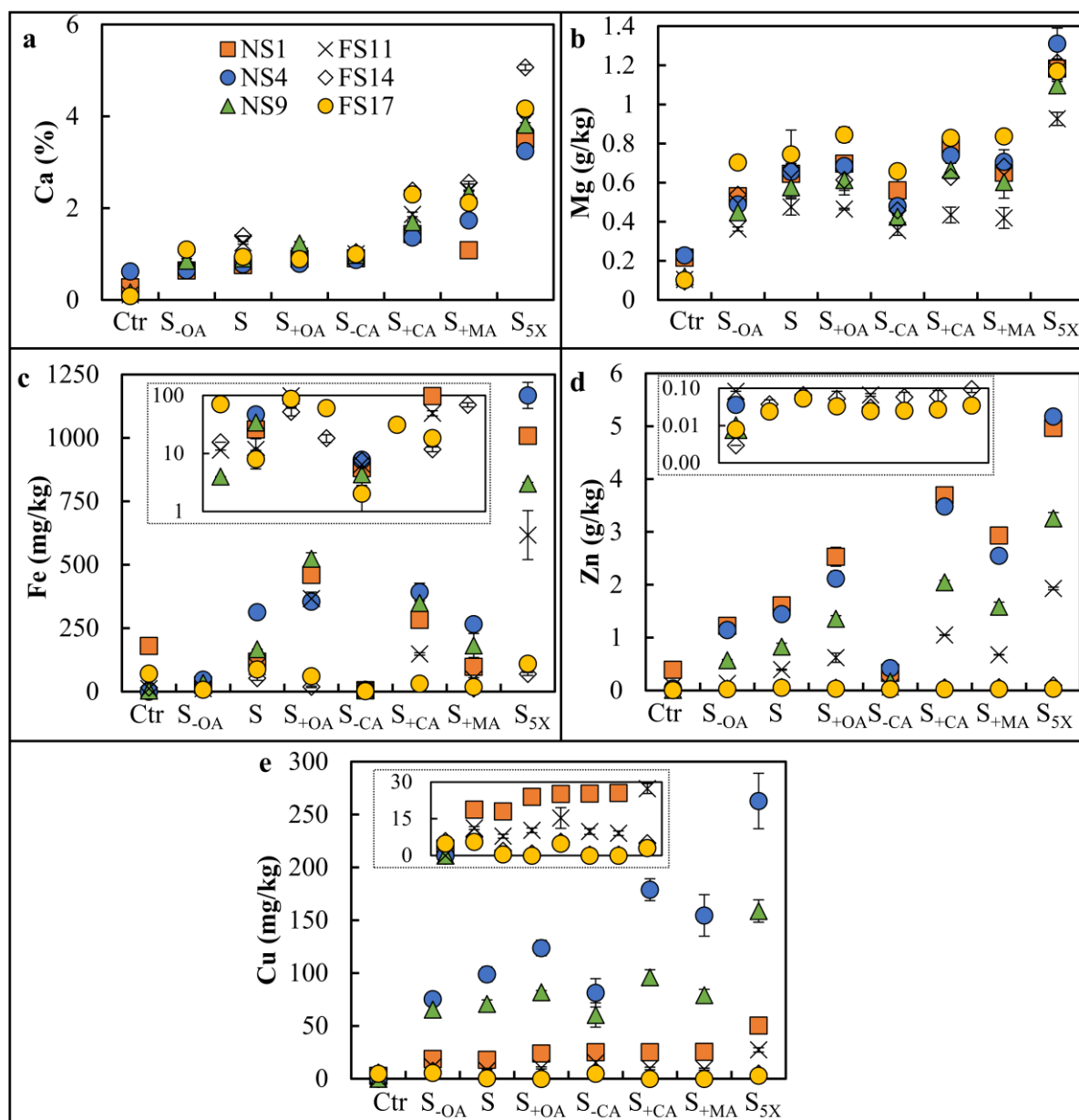


Fig. 2 The release of a) Ca (%), b) Mg (g/kg), c) Fe (mg/kg), d) Zn (g/kg), and e) Cu (mg/kg) from the technosols induced by SRE. The insets in c-e highlight the low metal release contents.

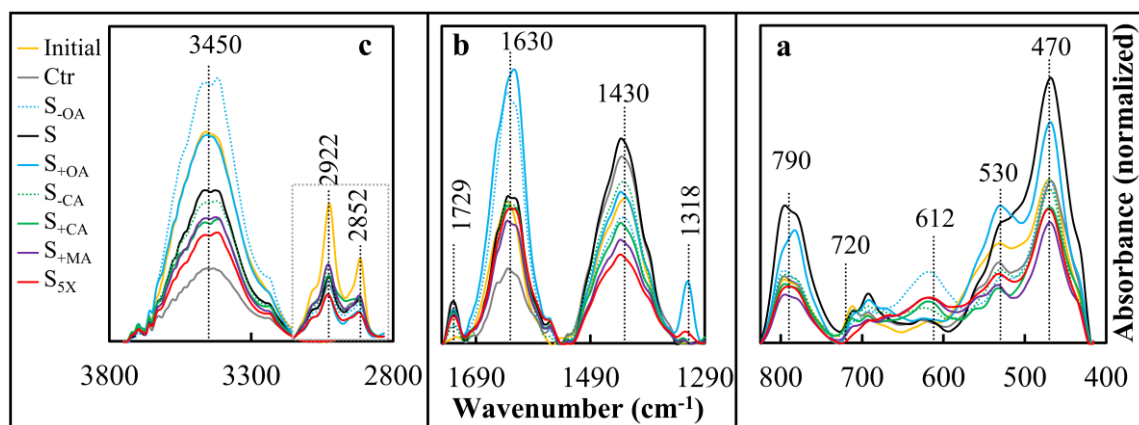


Fig. 3 FTIR spectra of the technosols after SRE treatments. The spectral regions are divided into 820-400 cm^{-1} (a), 1740-1290 cm^{-1} (b), and 3750-2800 cm^{-1} (c). The spectra in the 3000-2800 cm^{-1} region are enlarged for better visualization. For convenience, the spectra of only NS1 are included. Unless stated otherwise in the text, the other technosols showed similar changes.

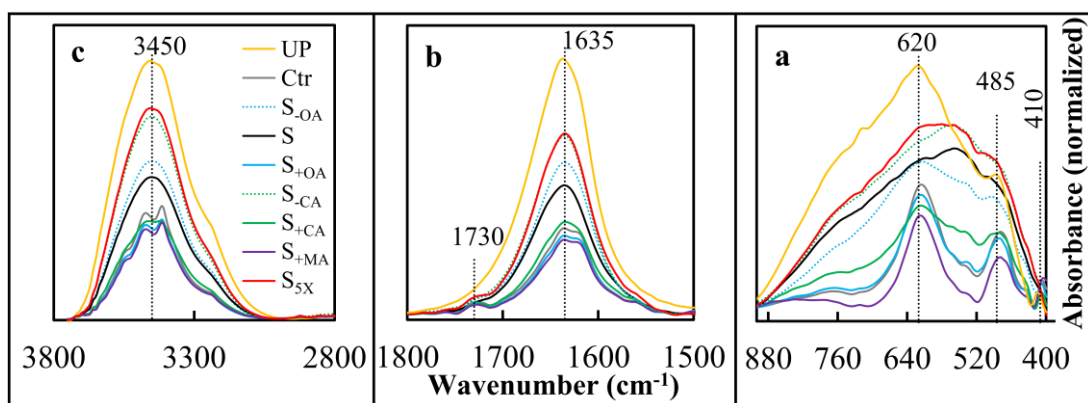


Fig 4. FTIR spectra of the liquid samples after the metal desorption experiment. The spectral regions are divided into 900-400 cm^{-1} (a), 1800-1500 cm^{-1} (b), and 3800-2800 cm^{-1} (c). For convenience, the spectra of only NS1 are included.

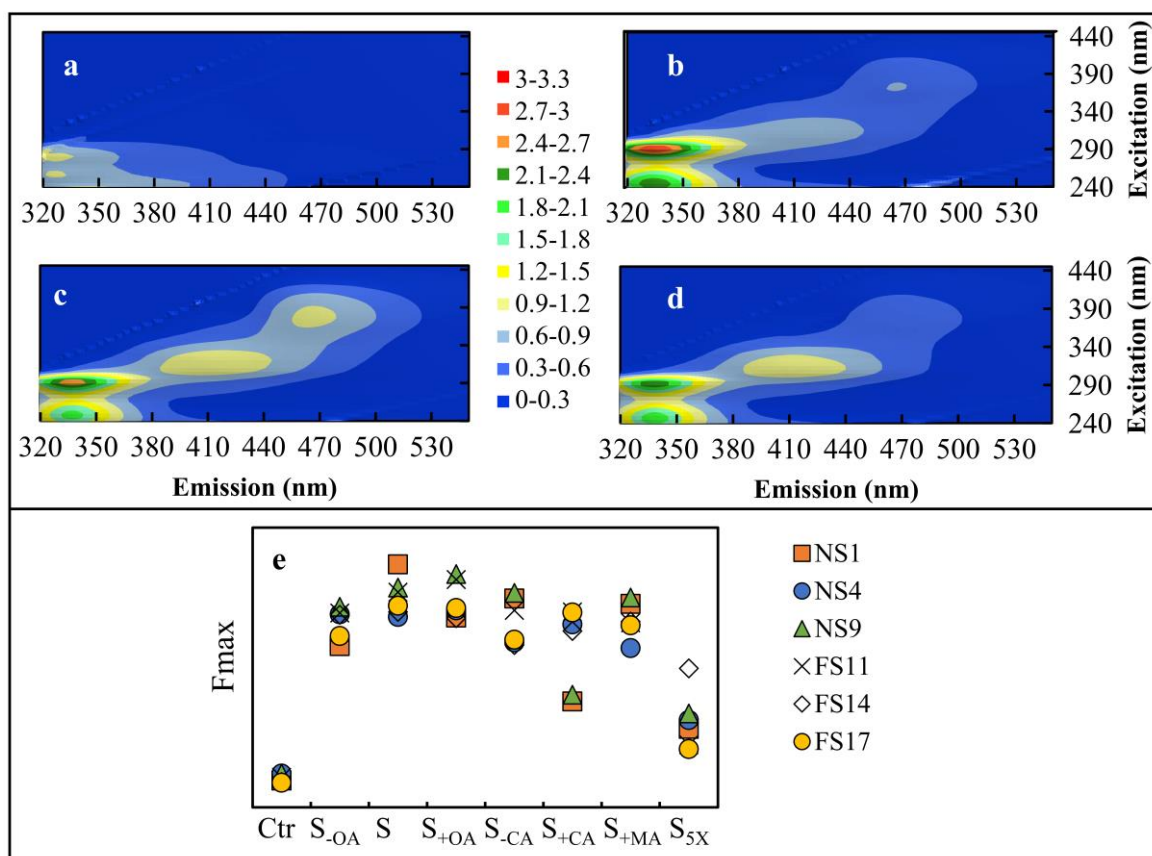


Fig 5. Excitation-emission matrices (EEM) of the solutions after the metal sorption experiment (a-d) and Fmax (e) for the second region (HA-like materials). The EEM of the control (a), S-0A (b), S (c), and S+0A (d) treatments of NS1 are shown. The data for the other samples and treatments are included in **Table S4**.

Appendix A. Supplementary data

Selective metal leaching from technosols based on synthetic root exudate composition

Hussein Jaafar Kanbar^{1,2,**}, Zeinab Matar^{1,3,4,**}, Ghina Safa^{1,3}, Veronique Kazpard^{1,3,4}

1. Research and Analysis Platform for Environmental Sciences (PRASE), Doctoral School of Sciences and Technology (EDST), the Lebanese University, P.O. 5, Rafic Hariri Campus, Hadat, Lebanon.
2. Department of Chemistry, Umeå University, SE-901 87, Umeå, Sweden.
3. Department of Earth and Life Sciences, Faculty of Sciences, the Lebanese University, Rafic Hariri Campus, Hadat, Lebanon.
4. Laboratory of Georessources, Geosciences and Environment (L2GE), Faculty of Sciences, the Lebanese University, Fanar, Lebanon.

Received 16 February 2020

Revised 13 April 2020

Accepted 24 April 2020

** These authors contributed equally to this work. Corresponding authors. E-mail: Hussein.kanbar@umu.se (H.J. Kanbar), z.matar@ul.edu.lb (Z. Matar).

 Hussein J. Kanbar <http://orcid.org/0000-0002-9505-9974>

Content

Table S1: The composition and concentrations of the synthetic root exudate components, and the structure and pKa values for the functional groups of the low molecular weight organic acids (LMWOAs).....	1
Table S2: The pH and EC (in $\mu\text{S}/\text{cm}$) values for the initial SRE solutions and the solutions after 24 hr mixing with technosols. The average values \pm standard deviations are included (n=3). For controls (Ctr, i.e., samples treated with ultrapure water), n=1	2
Table S3: Total metal content, oxalate extractable metal content, and percentage of oxalate extractable metals of the technosols (Kanbar et al., 2018).....	3
Table S4: Maximum fluorescence intensities (Fmax) for the SRE solutions after mixing with the technosols. Control indicates the technosols treated with ultrapure water.....	4
Fig. S1: Correlations between Mg and Ca release and electric conductivity “EC” (a) and the correlation between Zn, Cu, and Fe release (b-d)	5
Fig. S2: Ratios of metal release according to different treatments	6
S1: Quality assurance and quality control (QA/QC) procedures	7

Table S1: The composition and concentrations of the synthetic root exudate components, and the structure and pKa values for the functional groups of the low molecular weight organic acids (LMWOAs)

The concentrations included in the table are those in the SRE-technosol mixture. The concentrations that mark the variation between the different SRE solutions are highlighted in yellow.

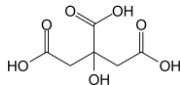
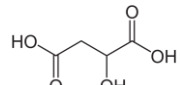
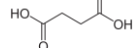
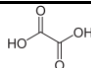
Component		Treatment							Structure	pKa (Kalka, 2019; Silva et al., 2009)	
		1	2	3	4	5	6	7		Group	Values
		S _{OA}	S	S _{OA}	S _{CA}	S _{CA}	S _{MA}	S _{5X}			
Concentrations (mmol/L) of the SRE components											
Sugar	Glucose.H ₂ O	0.5	0.5	0.5	0.5	0.5	0.5	2.5			
	D-Fructose	0.5	0.5	0.5	0.5	0.5	0.5	2.5			
	Sucrose	0.5	0.5	0.5	0.5	0.5	0.5	2.5			
Low molecular weight organic acids (LMWOAs)	Citric acid	0.25	0.25	0.25	0	1.25	0.25	1.25		Carboxyl	pKa ₁ 3.1 pKa ₂ 4.8 pKa ₃ 6.4
										Hydroxyl	pKa 14.4
	Malic acid	0.25	0.25	0.25	0.25	0.25	1.25	1.25		Carboxyl	pKa ₁ 3.4 pKa ₂ 5.2
										Hydroxyl	pKa 14.5
	Succinic acid	0.25	0.25	0.25	0.25	0.25	0.25	1.25		Carboxyl	pKa ₁ 4.2 pKa ₂ 5.6
	Oxalic acid	0	0.25	1.25	0.25	0.25	0.25	1.25		Carboxyl	pKa ₁ 1.3 pKa ₂ 4.3
Sum of LMWOAs		0.75	1	2	0.75	2	2	5			
Amino acids	DL-Serine	0.125	0.125	0.125	0.125	0.125	0.125	0.625			
	L-Leucine	0.125	0.125	0.125	0.125	0.125	0.125	0.625			
	L-Proline	0.125	0.125	0.125	0.125	0.125	0.125	0.625			
Phenolic acid	Trans-Cinnamic acid	0.125	0.125	0.125	0.125	0.125	0.125	0.625			
	Vanillic acid	0.125	0.125	0.125	0.125	0.125	0.125	0.625			
	Trans-Ferulic acid	1.25	1.25	1.25	1.25	1.25	1.25	6.25			

Table S2: The pH and EC (in $\mu\text{S}/\text{cm}$) values for the initial SRE solutions and the solutions after 24 hr mixing with technosols. The average values \pm standard deviations are included (n=3). For controls (Ctr, i.e., samples treated with ultrapure water), n=1

Solution	Initial pH	pH of solutions after 24 hr					
		NS1	NS4	NS9	FS11	FS14	FS17
Ctr	8.64	7.86	8.03	7.43	8.20	8.76	8.06
Treatment	S _{OA}	6.07 \pm 0.09	6.36 \pm 0.03	6.46 \pm 0.02	6.58 \pm 0.03	6.68 \pm 0.02	6.78 \pm 0.02
	S	7.45 \pm 0.03	7.33 \pm 0.05	7.42 \pm 0.03	7.76 \pm 0.16	7.89 \pm 0.01	7.90 \pm 0.01
	S _{OA}	6.81 \pm 0.14	6.80 \pm 0.07	6.88 \pm 0.03	7.07 \pm 0.02	7.32 \pm 0.15	6.57 \pm 0.01
	S _{CA}	6.27 \pm 0.05	6.41 \pm 0.02	6.46 \pm 0.01	6.52 \pm 0.03	6.63 \pm 0.03	6.72 \pm 0.00
	S _{CA}	6.57 \pm 0.02	6.47 \pm 0.01	6.54 \pm 0.07	6.84 \pm 0.11	6.96 \pm 0.11	7.36 \pm 0.23
	S _{MA}	6.99 \pm 0.09	6.12 \pm 0.09	6.67 \pm 0.03	6.77 \pm 0.04	6.92 \pm 0.07	7.06 \pm 0.01
	S _{5X}	6.78 \pm 0.06	6.35 \pm 0.01	6.47 \pm 0.01	6.43 \pm 0.02	6.55 \pm 0.10	6.73 \pm 0.02

Solution	Initial EC ($\mu\text{S}/\text{cm}$)	EC ($\mu\text{S}/\text{cm}$) of solutions after 24 hr					
		NS1	NS4	NS1	FS11	NS1	FS17
Ctr	80	102	131	109	72	71	76
Treatment	S _{OA}	321 \pm 12	318 \pm 3	355 \pm 10	322 \pm 7	338 \pm 10	324 \pm 3
	S	391 \pm 5	349 \pm 8	399 \pm 3	408 \pm 15	356 \pm 4	347 \pm 5
	S _{OA}	409 \pm 29	376 \pm 6	436 \pm 9	442 \pm 15	510 \pm 45	405 \pm 8
	S _{CA}	337 \pm 23	313 \pm 15	325 \pm 12	298 \pm 7	300 \pm 6	301 \pm 6
	S _{CA}	519 \pm 34	475 \pm 39	524 \pm 23	483 \pm 12	526 \pm 5	504 \pm 1
	S _{MA}	547 \pm 12	487 \pm 2	568 \pm 9	496 \pm 6	538 \pm 11	495 \pm 9
	S _{5X}	831 \pm 35	777 \pm 42	818 \pm 38	745 \pm 28	843 \pm 35	724 \pm 16

Table S3: Total metal content, oxalate extractable metal content, and percentage of oxalate extractable metals of the technosols (Kanbar et al., 2018)

	Ca			Mg			Fe			Zn			Cu		
Sample	Tot (%)	OxEx (%)	% Ox/Tot	Tot (%)	OxEx (%)	% Ox/Tot	Tot (%)	OxEx (%)	% Ox/Tot	Tot (mg/kg)	OxEx (mg/kg)	% Ox/Tot	Tot (mg/kg)	OxEx (mg/kg)	% Ox/Tot
NS1	11.6	-	-	2.9	0.3	9.1	12.3	5.7	45.9	22143	12463	56	434	263	61
NS4	9.6	-	-	2.7	0.2	7.7	20.0	16.0	79.8	12562	7897	63	2745	1023	37
NS9	8.5	-	-	0.4	0.2	41.0	23.7	16.9	71.0	15391	8701	57	3060	848	28
FS11	10.9	-	-	0.9	0.6	63.6	3.6	2.9	80.8	6018	5329	89	159	87	54
FS14	9.7	-	-	0.9	0.5	49.6	3.4	0.5	15.6	459	267	58	28	16	57
FS17	3.1	-	-	0.7	0.1	20.6	5.4	0.3	5.7	87	67	78	28	8	27

Tot: total metal content
OxEx: oxalate extractable metal content
% Ox/Tot: the percentage of oxalate extractable metal divided by the total metal multiplied by 100.

The bold characters highlight % Ox/Tot of samples with the highest metal release (more information is found in the main text). Ferriallophanes are identified by high oxalate extractable Fe out of total Fe contents (i.e., high % Ox/Tot).

Table S4: Maximum fluorescence intensities (Fmax) for the SRE solutions after mixing with the technosols. Control indicates the technosols treated with ultrapure water

Sample	Treatment	1 st region		2 nd region
		Peak1	Peak2	Peak3
		$\lambda_{ex}/\lambda_{em} = 245\text{-}250/338 \text{ nm}$	$\lambda_{ex}/\lambda_{em} = 290\text{-}295/338 \text{ nm}$	$\lambda_{ex}/\lambda_{em} = 260\text{-}420/380\text{-}500 \text{ nm}$
NS1	Control	800	936	241
	S-OA	2352	3006	1016
	S	1892	2596	1797
	S+OA	1969	2299	1376
	S-CA	1334	1238	1596
	S+CA	2228	2706	634
	S+MA	1733	2072	1487
	S _{5X}	77	60	489
NS4	Control	1391	1510	303
	S-OA	2661	3223	1301
	S	1408	2074	1328
	S+OA	2766	3807	1441
	S-CA	1767	1567	1204
	S+CA	1332	1987	1322
	S+MA	1606	3304	1092
	S _{5X}	31	22	568
NS9	Control	1949	2047	301
	S-OA	2118	2169	1366
	S	1976	2221	1589
	S+OA	2380	2843	1763
	S-CA	1393	1530	1644
	S+CA	1711	2490	693
	S+MA	1157	1308	1543
	S _{5X}	106	91	625
FS11	Control	1841	1942	268
	S-OA	1691	1589	1309
	S	1853	1813	1546
	S+OA	1875	1920	1715
	S-CA	1834	1706	1488
	S+CA	1515	1783	1432
	S+MA	1469	1629	1316
	S _{5X}	54	44	344
FS14	Control	2376	2382	227
	S-OA	2865	2235	1295
	S	2130	2102	1369
	S+OA	1699	1566	1369
	S-CA	1136	1025	1179
	S+CA	1227	1233	1262
	S+MA	1438	1372	1327
	S _{5X}	80	59	1027
FS17	Control	464	721	222
	S-OA	1787	1893	1106
	S	1784	1941	1427
	S+OA	1818	1649	1462
	S-CA	1370	1260	1227
	S+CA	2054	2173	1430
	S+MA	1414	1466	1295
	S _{5X}	127	92	309

Fig. S1: Correlations between Mg and Ca release and electric conductivity “EC” (a) and the correlation between Zn, Cu, and Fe release (b-d)

The change in EC was mainly dependent on the release of the major cations (Ca and Mg), as seen by strong correlations between each metal and EC (R^2 values in part “a” of the figure). Furthermore, the release of Mg and Ca is strongly correlated to the concentrations of the low molecular weight organic acids (LMWOAs) in the synthetic root exudate (SRE) solutions. On the other hand, the release of Fe, Zn, and Cu largely depended on the technosols (and less on the SRE solution). For example, Cu-Fe and Cu-Zn were correlated between two groups of technosols, which are NS4-NS9 and the other samples (NS1 and FS technosols). As for Zn-Fe, they were correlated between two other groups, which are all the NS samples and FS11 (group 1) and FS14 and FS17 (group 2). This highlights that in addition to the role of LMWOAs, metal behavior is largely dependent on the characteristics of technosols.

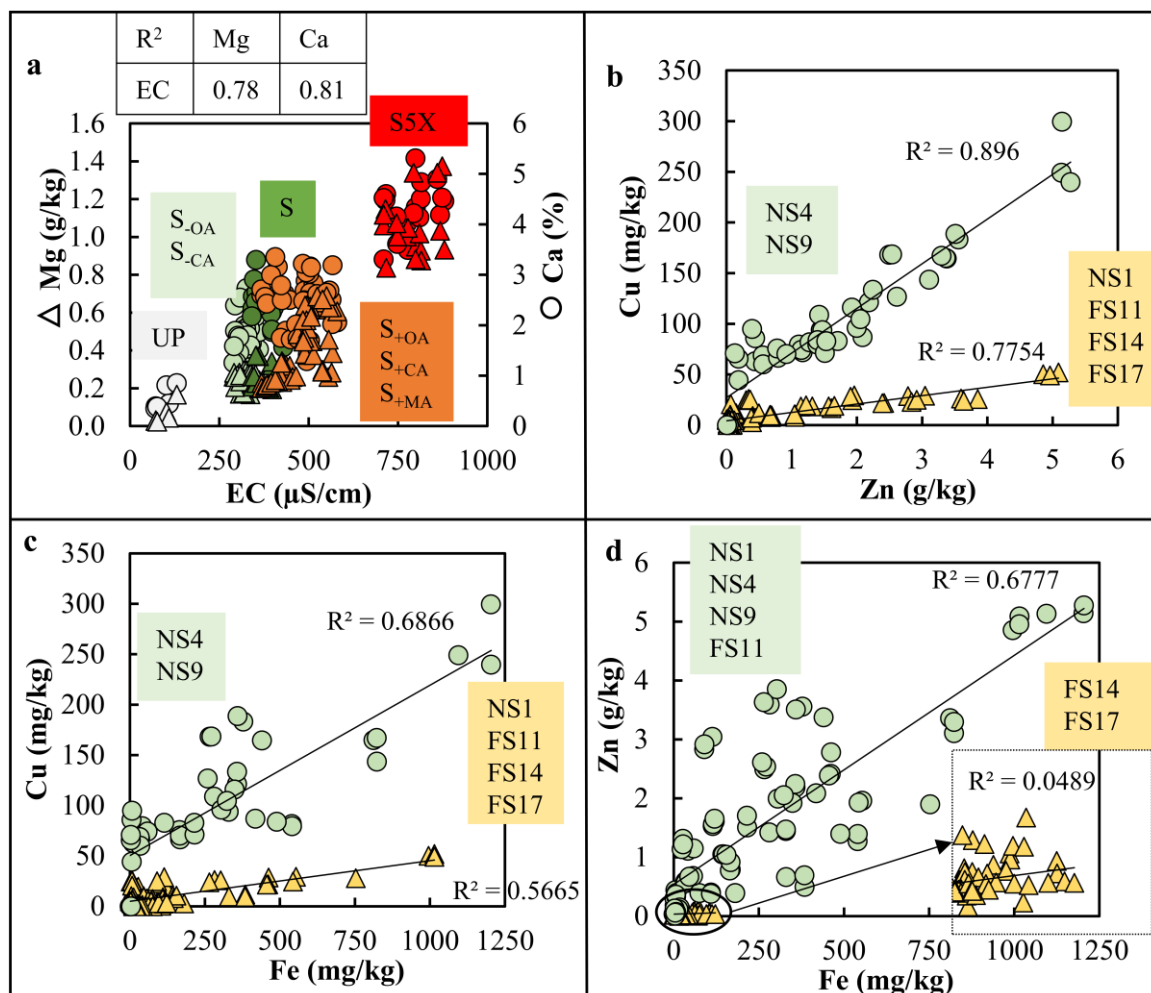
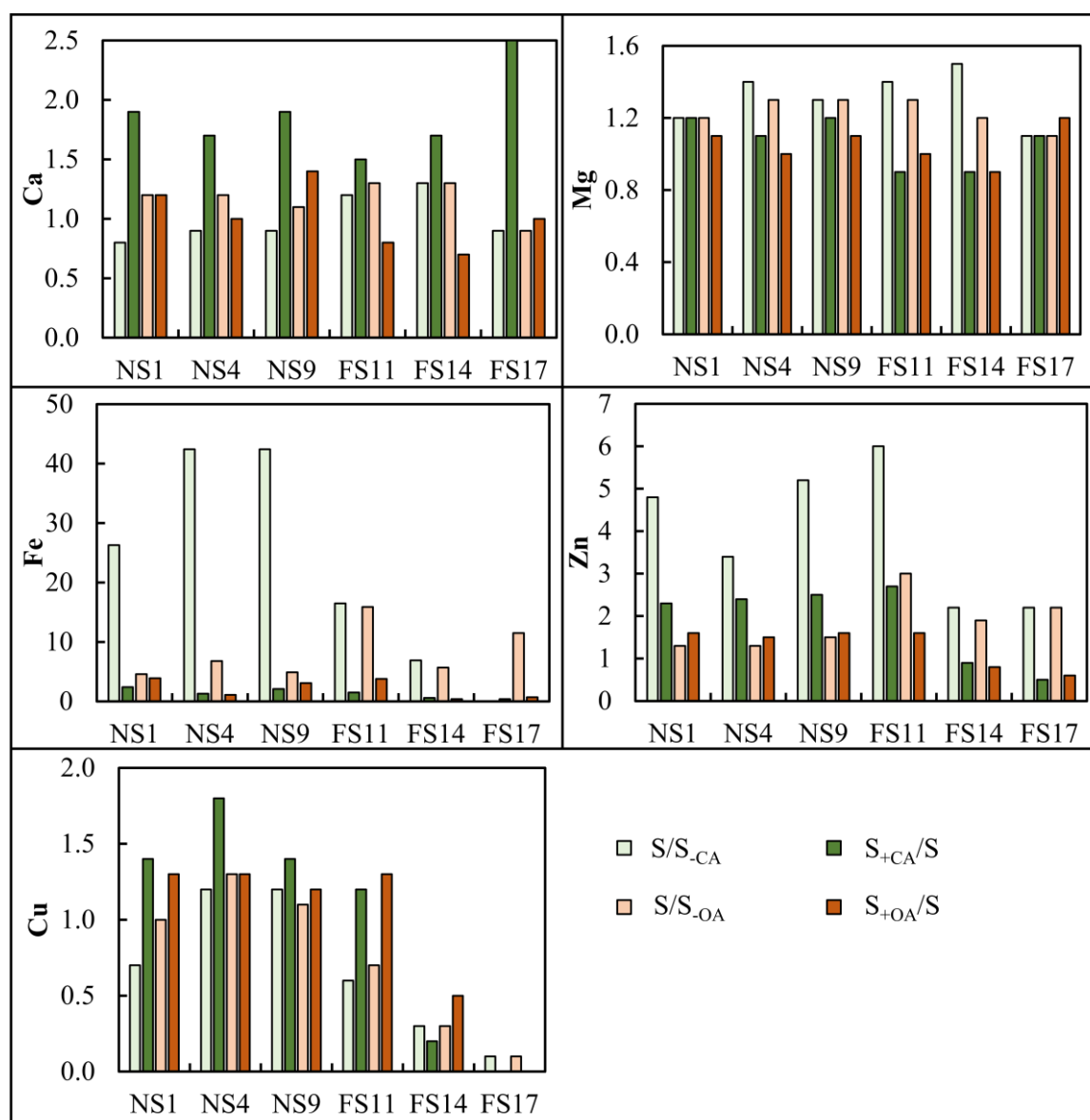


Fig. S2: Ratios of metal release according to different treatments

Ratios of metal release were used for a clearer visualization of the link between the influence of low and high concentrations of LMWOAs. For example, S/S_{-CA} highlighted the role of relatively low concentrations of CA (0-0.25 mmol/L) and S_{+CA}/S highlighted the role of relatively high concentrations of CA (0.25-1.25 mmol/L). In the case of Zn, $Zn\ S/S_{-CA} > S_{+CA}/S$. So, Zn release by SRE was more prominent when CA concentrations were relatively low; under higher concentrations of CA (0.25-1.25 mmol/L), Zn release was less prominent.



S1: Quality assurance and quality control (QA/QC) procedures

QA/QC procedures were implemented based on external standards. Those standards were also used for calibration. Accuracy and reproducibility of the measurements were validated by running the external standards between every ~10 samples. The values were taken unless the error exceeded 5-10%. The quantification and detection limits (LOQ and LOD, respectively) were calculated according to the ICH Harmonized Tripartite Guideline (ICH Harmonized Tripartite Guideline, 2005).

References

- ICH Harmonized Tripartite Guideline, 2005. Validation of analytical procedures: text and methodology Q2 (R1), in: International Conference on Harmonization of Technical Requirements for Registration of Pharmaceuticals for Human Use. Geneva, Switzerland, p. 13.
- Kalka, H., 2019. Organic Acids and Salts [WWW Document]. Aqion. URL <https://www.aqion.de/site/189#pK> (accessed 12.14.19).
- Kanbar, H.J., Srouji, E.E., Zeidan, Z., Chokr, S., Matar, Z., 2018. Leaching of metals in coastal technosols triggered by saline solutions and labile organic matter removal. *Water, Air, Soil Pollut.* 229, 157. <https://doi.org/10.1007/s11270-018-3808-z>
- Silva, A.M.N., Kong, X., Hider, R.C., 2009. Determination of the pKa value of the hydroxyl group in the α -hydroxycarboxylates citrate, malate and lactate by ^{13}C NMR: implications for metal coordination in biological systems. *BioMetals* 22, 771–778. <https://doi.org/10.1007/s10534-009-9224-5>